Laser and Particle Beams (2006), *24*, 95–100. Printed in the USA.

DOI: 10.1017/S0263034606060149

Monoenergetic electron beam generation from a laser-plasma accelerator

K. KOYAMA,[1,4] M. ADACHI,[2] E. MIURA,[1] S. KATO,[1] S. MASUDA,[3] T. WATANABE,[4] A. OGATA,[2] AND M. TANIMOTO[5]

[1]National Institute of Advanced Industrial Science and Technology (AIST), Tsukuba, Japan
[2]Graduate School of Advanced Sciences of Matter, Hiroshima University, Higashi-Hiroshima, Japan
[3]National Institute of Radiological Sciences (NIRS), Chiba, Japan
[4]Graduate School of Engineering, Utsunomiya University, Utsunomiya, Japan
[5]Faculty of Physical Sciences and Engineering, Meisei University, Hino, Japan

(RECEIVED 17 May 2005; ACCEPTED 19 September 2005)

Abstract

We have demonstrated the acceleration of a monoenergetic electron beam by a laser-produced wakefield. Experiments were performed by focusing 2-TW laser pulses of 50 fs on supersonic gas-jet targets. The focused intensity was 5×10^{18} W/cm^2 ($a_0 = 1.5$). At an electron density of 1.5×10^{20} cm^{-3}, the clear monoenergetic electron beam from the plasma was obtained at 7 to 15 MeV. The Stokes satellite peak in the forward scattering explained the energy spectra of electrons at various plasma densities well. Although the wakefield propagated 500 microns, which was far beyond the dephasing length, monoenergetic electron beams were obtained.

Keywords: Dephasing; Forward scattering; Laser plasma accelerator; Monoenergetic acceleration; Self-modulated wakefield

1. INTRODUCTION

The recent compact terawatt laser systems deliver focused intensities approaching 10^{20} W/cm^2, while petawatt lasers are expected to attain intensities beyond 10^{21} W/cm^2 in the near future. High-intensity laser-plasma interactions are of considerable interest because of the relevant physics of compact accelerators, the ignition of inertial confinement fusion, and astrophysics. In the past few years, electrons accelerated by relativistic plasma waves excited by intense laser pulses have reached the maximum energy over 100 MeV. However, the energy spectra have been similar to the Mawellian distribution, that is, the energy spread was almost 100% (Malka *et al.*, 2002). Although some applications of the laser plasma particle accelerators are studied (Malka & Fritzler, 2004; Mangles *et al.*, 2004), one of the crucial problems in realizing a laser plasma particle accelerator has been with regard to the acceleration of the monoenergetic electron beam at a low emittance.

After the suggestive experiment performed by at the National Institute of Advanced Industrial Science and Technology (AIST), which showed an electron beam with a quasi-monoenergetic peak at approximately 6 MeV (Koyama *et al.*, 2003), some experiments on monoenergetic electron acceleration were reported (Faure *et al.*, 2004; Geddes *et al.*, 2004; Glinec *et al.*, 2005; Koyama *et al.*, 2004). However, the reproducibilities were rather poor. In order to achieve the good reproducibility of the monoenergetic acceleration, plasmas as well as laser pulses should be carefully controlled. We have recently obtained a clear monoenergetic peak by using plasma diagnostic techniques to find suitable conditions (Miura *et al.*, 2005). Experiments were performed at an electron density of approximately 10^{20} cm^{-3} in order to excite a moderately large amplitude of a wakefield by a relatively small laser power of 2 TW and to guide the laser pulse by the relativistic self-focusing beyond the Rayleigh length.

In our experiment, monoenergetic electron beams were observed in a narrow region of electron density that lay between the density range of no-acceleration and acceleration to the energy spectra of continuum. The correlation between the forward scattering spectra of laser light and the energy spectra of electron beams suggests that the monoenergetic beam was accelerated by the self-modulated wakefield.

Address correspondence and reprint requests to: K.Koyama, National Institute of AIST, Tsukuba Central-2,1-1-1,Umezono, Tsukuba, Ibaraki, 305-8568 Japan. E-mail: k.koyama@aist.go.jp

2. EXPERIMENT

Experiments were performed at AIST with a Ti:sapphire laser operating at a wavelength of 800 nm. The laser delivered a pulse energy of 100 mJ in 50-fs full width at half maximum (FWHM) with a linear polarization. As schematically shown in Figure 1, a laser pulse was focused by an f/3.5 off-axis parabolic mirror on a supersonic gas jet, which was ejected into a vacuum. One-half of the laser energy was contained in a focal spot diameter of 5 μm FWHM (a Gaussian-beam waist was $w_0 = 4.3$ μm). The vacuum-focused intensity was 5×10^{18} W/cm^2, for which the corresponding normalized vector potential was $a_0 = 1.5$. A confocal length, which is twice the Rayleigh length, is estimated to be 140 μm. The contrast ratio of the main pulse to the prepulse preceding it by 5 ns was 10^{-4}.

In order to produce a plasma, a nitrogen (N_2) gas and a helium (He) gas were ejected from a supersonic conical nozzle fed by a pulsed gas valve (General Valve: Series 9). The diameters of the nozzle exit were chosen around 1 mm to obtain an electron density higher than 10^{20} cm^{-3}. Mach numbers of nozzles were chosen ranging from 3 to 5 for varying the density gradient of gas jets. Neutral density profiles of gas jets were characterized by using the interferometer. When the reservoir pressure of the gas valve was 3 MPa (30 bar), the molecular density of N_2 gas on the central axis of the gas jet was 1.5×10^{19} cm^{-3} at 1 mm from the nozzle exit. The electron density is estimated to be 1.5×10^{20} cm^{-3} by the barrier suppression ionization (BSI) model (Augst *et al.*, 1989) for our laser intensity. For producing the dense He gas jet of 7×10^{19} cm^{-3}, the gas valve was operated at a reservoir pressure of 8 MPa. Differences between the gas constants as well as the ionization potentials between the gas species enable us to study the influence of the ionization refraction at different density gradients.

The spectra of electrons accelerated by laser-produced plasmas were measured by using an electron spectrometer (ESM) on the optical axis of the laser. Electrons collimated by an entrance slit entered a magnetic field, in which they were dispersed energetically along the side where the imaging plate (IP, Fujifilm Co.: BAS-SR) was placed. The stray visible light was blocked by a 15-μm-thick aluminum foil. The width and height of a slit of the ESM were 3 mm and 7 mm, respectively. The IP ensured that an angle resolved energy spectrum of an electron beam could be recorded. A uniform magnetic field of 0.2 T was generated by a pair of permanent magnets. The ESM had electron energy coverage from 0.2 to 30 MeV. The entire spectrometer was placed in an iron box to decrease stray magnetic field between the plasma and the ESM. The strength of the stray field at the outer side of the slit was smaller than 3 mT. For the estimation of the number of accelerated electrons, we used the calibrated sensitivity of the IP (Takahashi *et al.*, 2002; Tanaka *et al.*, 2005).

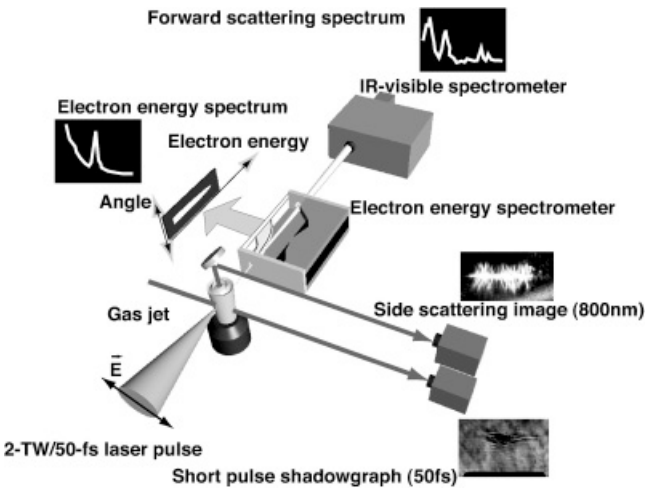

Fig. 1. The schematic drawing of the experimental layout.

In order to clarify the mechanisms of electron acceleration, the spectra of forward scattering by the plasmas were measured from the outer side of the vacuum chamber through the viewing holes of the ESM, as shown in Figure 1. A spectrometer and a Si-photodiode array detector covered a wavelength range from 650 to 1100 nm. In order to avoid the saturation of the Si-detector around the laser wavelength of 800 nm, a laser-mirror was placed in front of the spectrometer. In order to eliminate a second-order diffraction of the short wavelength scattering light, we used a color glass filter that cut the wavelength that was shorter than 670 nm.

In addition to the measurement of the spectrum of the forward scattering, a side-scattering image of the pump laser pulse was observed from a normal direction to the polarization vector. A narrow band interference filter at a wavelength of 800 nm, neutral density (ND) filters and a polarizing filter were used to cut a self-emission (recombination emissions) from the plasma and analyze polarization, respectively. A common type of charge coupled device (CCD) camera was used to record the side-scattering.

A short-pulse shadow graph of the plasma was also used to monitor the propagation of the laser pulse and the density distribution of the plasma. The wavelength and the duration of the probe pulse were 800 nm and 50 fs, respectively. The shadow graph was usually monitored immediately after the main pulse passed through the plasma, which corresponded to a delay time of 6 ps from the focal point. The shadow graph was monitored once in a while at a few nanoseconds before the main pulse in order to examine the influence of the prepulse on the pre-plasma production.

3. RESULTS

Neither were the obvious signs of pre-plasma production recorded in the shadowgraph nor was the obvious influence on the electron energy spectrum was observed at the contrast ratio of the prepulse of 10^{-4}. When the prepulse contrast was increased to 10^{-3}, the cylindrical expansion of the preformed plasma was observed and the high-energy com-

ponent of the energy spectrum of electrons disappeared. A typical energy spectrum of the monoenergetic electron beam obtained by 90-shot integration on the IP is shown in Figure 2a. This was obtained at a reservoir pressure of 3 MPa ($n_e \approx 1.5 \times 10^{20}$ cm^{-3}). A small spot in the IP image at approximately 7 MeV indicates the monoenergetic electron beam. The divergence angle of a monoenergetic beam of $\gamma = 14$ (7 MeV) was $\delta\theta \approx \pm 1.2°$. Supposing that the source diameter of the electron beam (2σ) was identical to the focus diameter of 5 μm, a normalized emittance ($\epsilon_n = \gamma\sigma\delta\theta$) of 0.7 πmm mrad was estimated, which is as small as that of modern accelerators. Figure 2b shows a line out of the IP image. The vertical axis is evaluated by using the sensitivity curve of the IP (Takahashi *et al.*, 2002; Tanaka *et al.*, 2005). The monoenergetic peak at 7 MeV is clearly shown. The observed energy spread (FWHM) of the peak was 2.5 MeV, which was blurred by the low resolving power of the ESM. Monoenergetic beams were obtained at a narrow density range of 1.1×10^{20} cm^{-3}–1.5×10^{20} cm^{-3}, as shown in Figure 3. Although the number of electrons drastically with the electron density to exceed 2×10^{20} cm^{-3}, the energy spectra of electrons were similar to the Maxwellian distribution, that is, no monoenergetic peak was observed. In the opposite density region of lower than 8×10^{19} cm^{-3}, no obvious high-energy acceleration was observed, as shown in Figure 4a. Since the number of shots with the He-jet was insufficient, it is difficult to evaluate the influence of the ionization refraction quantitatively. One of the results clearly indicates that the energy gain of the electron beam is a function of the electron density, independent of the atomic number of the gases.

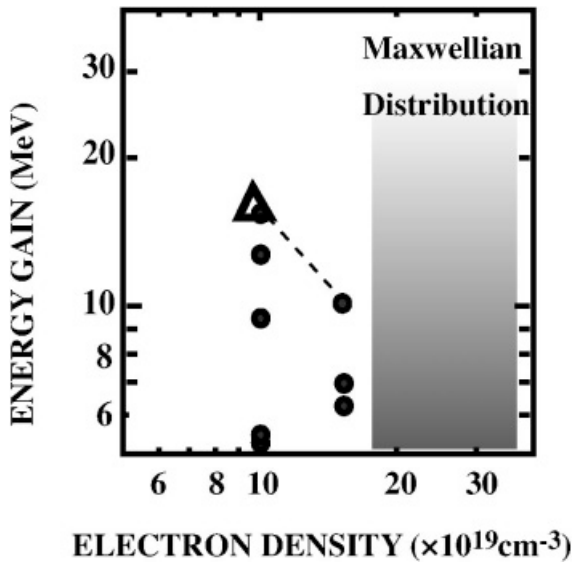

Fig. 3. Energy gain of monoenergetic peaks for different electron densities. The density region of the Maxwellian energy spectra is indicated by the shaded area. The open triangle was produced by the He-plasma. Others were accelerated in N-plasmas.

The forward scattering spectra of the laser light from the plasma varied with changes in the electron density, as shown in Figure 4b. The amplitude and the wavelength of the first Stokes satellite peak of the forward scattering of around 1000 nm became larger and longer, respectively, with an increase in electron density from 10^{20} cm^{-3} to 1.5×10^{20} cm^{-3}. Following this, the satellite became a broad plateau at a density higher than 2×10^{20} cm^{-3}. Supposing that the forward scattering spectra were caused by the Raman scattering, the electron density was estimated to be (1.3 to 1.5) $\times 10^{20}$ cm^{-3} from the wavelength of the satellite peak by considering the relativistic effect on the plasma fre-

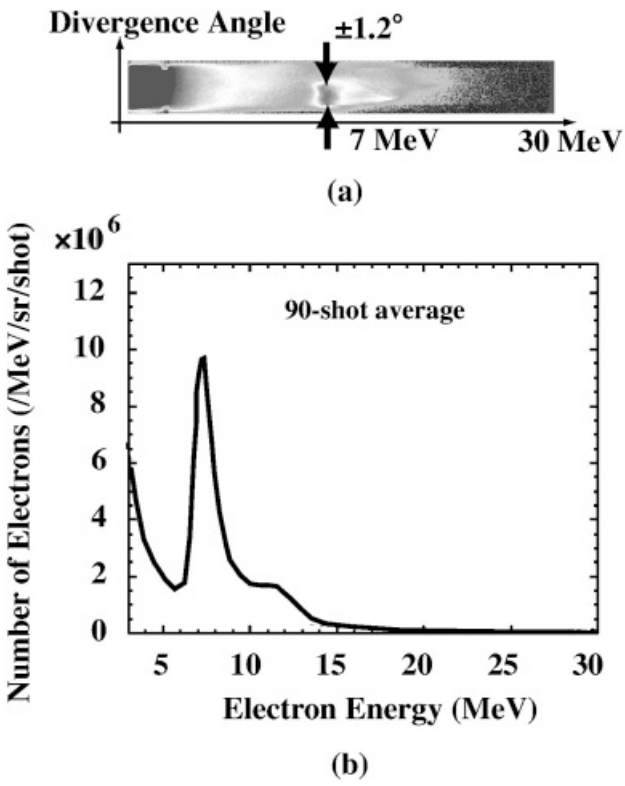

Fig. 2. The IP-image of the angle-resolved energy spectrum after 90-shots integration (**a**) and the deduced energy spectrum (**b**).

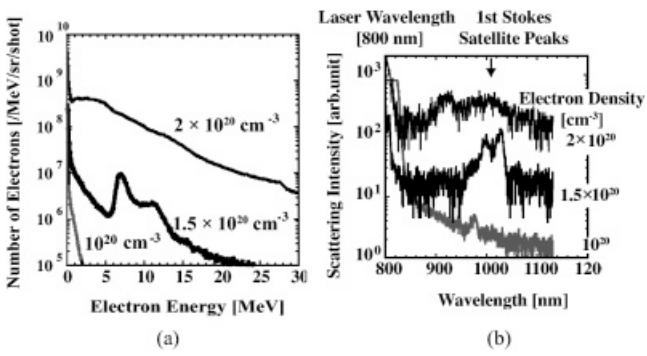

Fig. 4. Electron energy spectra (**a**) and forward scattering spectra of the laser light (**b**) for different electron densities.

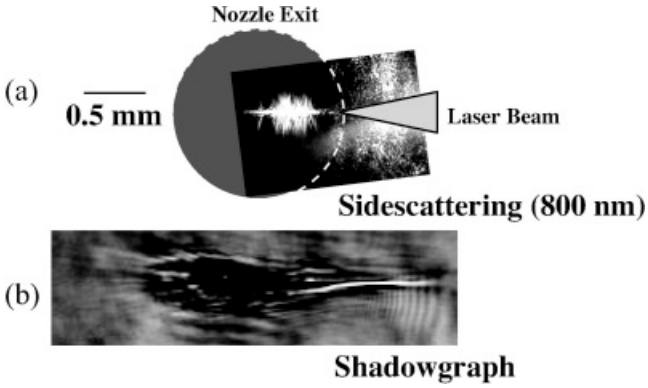

Fig. 5. The side scattering image at the laser wavelength (**a**) and the shadowgraph (**b**).

quency at $a_0 = 1.5$, which was consistent with the density estimated from the measured density of the neutral gas.

Figure 5a shows a typical side-scattering image of the laser light from the plasma. The appearance of the fishbone structure of the side scattering was well correlated with the appearance of the first Stokes satellite of the forward scattering. The length of the fishbone structure was approximately 500 μm, which terminated near the center of the gas jet. The intensity of the side scattering light is sufficiently high as to be detectable by a CCD camera with ND-filters. The polarization of the scattering light conserved that of the incident laser pulse. This suggests that the intense side scattering was a coherent scattering from the plasma wave.

As shown in Figure 5b, the shadow graph, which is related to the density distribution of electrons, shows the track of the channeling followed by the breakup to many filaments after the point of termination of the fishbone structure.

4. DISCUSSION

The plasma density of our experiment was high to such an extent that the necessary condition of the self-modulated laser wakefield acceleration (SMLWFA) regime was satisfied; according to the condition, the product of electron plasma frequency ($\omega_p/2\pi$) and the width of the laser pulse (τ_L) should be greater than unity ($\omega_p\tau_L > 2\pi$), where the plasma frequency includes a relativistic effect.

The experimentally-obtained density dependence of the wavelength shift and the amplitude of the first Stokes satellite peak of the forward scattering provided clear evidence that the electron plasma wave was excited by the self-modulation of the laser pulse, that is, by the forward Raman instability. A comparison of the density dependence of electron energy spectra and the forward scattering spectra of Figure 4 clearly revealed that energy spectra of electrons were strongly connected with the plasma wave. The plasma wave excited in the high-density plasma underwent wave breaking, following which the electrons formed the energy spectrum of the continuum.

The growth and the amplitude of plasma wave were dependent on the seeding of the initial plasma wave, which might be dominated by the ionization effect (Mori & Katsouleas, 1992). Supposing the amplitude of the seeding wave to be approximately $10^{-4} \sim 10^{-3}$, the amplitude of the plasma wave after passing through several tens microns is roughly calculated to be 30–40%, where the growth rate of the forward Raman instability of $\gamma_{FRS} = (\omega_p^2/\sqrt{8}\omega_L) \times (a_0/\sqrt{1 + a_0^2/2})$ is used for the estimation. In the high density case of 2×10^{20} cm^{-3}, the wave amplitude simply calculated exceeds unity. However, no longitudinal wave-breaking occurs due to the relativistic plasma waves. The initial electrons might be supplied by the transverse wave-breaking of plasma waves of a finite radius (Bulanov *et al.*, 1997). For the low density case of 10^{20} cm^{-3}, the wave amplitude is sufficiently small. These tendencies are qualitatively identical to the observed spectra of the forward scattering.

The maximum acceleration energy is expressed by $\gamma_{max} = 2\gamma_{ph}^2(\delta n_e/n_0)$, where $\gamma_{ph} = (1 - v_{ph}^2/c^2)$ and v_{ph} is the phase velocity of the plasma wave that includes the relativistic effect and c is the speed of light. By using $\gamma_{ph} \approx 4.2$ for the plasma density of 1.5×10^{20} cm^{-3} and the wave amplitude of approximately 40%, the energy gain of the electron is estimated to be 7 MeV. This is close to the observed monoenergetic energy. Furthermore, the density dependence of the monoenergetic energy of n_e^{-1} is consistent with the experimental result, as shown in Figure 3.

The electron density of our experiment of 10^{20} cm^{-3} was sufficiently high to guide the laser pulse of 2 TW well beyond the Rayleigh length by the relativistic self-guiding and cause growth of the plasma wave to a large amplitude. The shadow graph showed a long track of the channeling before the breakup of the laser pulse. The channeling length did not necessarily coincide with that of the the acceleration. We estimated the propagation length of the plasma wave in the following manner. The relation between the fishbone structure in the side scattering and the plasma wave was previously discussed by Chen *et al.* (2000). Based on the preliminary estimation of the scattering intensity, it can be said that the intense side scattering might be due to the coherent scattering by the plasma wave with the density modulation of several to a few tens percents. The polarization of the side scattering light conserved that of the incident laser pulse. Based on the characteristics of the side scattering and the good correlation between the monoenergetic acceleration and the plasma wave, it can be stated that the propagation length of the plasma wave agreed with the length of the strong side scattering of 500 μm. Although the propagation length of the plasma wave was considerably longer than the dephasing length ($L_{dp} = 2\pi c\omega_L^2/\omega_p^3$) of 30 to 50 μm, the long propagation length could be regarded to be equivalent to the dephasing length provided that the propagation length is approximately an odd multiple of the dephasing length. The large spread of the energy gain is primarily due to the fluctuation of the outgoing phase of the electron

bunch from the wakefield. The acceleration length, which was terminated by the breakup of the laser pulse, was varied from shot to shot and was considerably longer than the dephasing length of the acceleration. In other words, if the propagation length of the wave is well controlled to coincide with the dephasing length, we can achieve a monoenergetic beam at a fixed energy with good reproducibility.

Although the above discussion was restricted to be one-dimensional (1D) effect, the tendency could be explained. If the 2D effect is included to explain the experiment, the motion of electrons in the plasma wave of a finite radius should be discussed. The dynamics of the electrons trapped and accelerated in plasma waves beyond the dephasing length has been reported (Chen *et al.*, 1999). When the trapped electrons enter the deceleration phase, the electrons with a large transverse momentum are pushed out from the region where the plasma waves are excited. At this point, the loss of the trapped electrons occurs. If the plasma waves are excited in a region far beyond the dephasing length, the loss of the trapped electrons can be repeated and it may limit the energy spread and the transverse angle spread. A small modulation around the Stokes satellite peak might be evidence of the electron trapping in the plasma wave (Kruer *et al.*, 1969).

We emphasize that the monoenergetic electron beam is accelerated by the large amplitude of the plasma wave, that dose not reach the longitudinal wavebreaking. The density of the monoenergetic electron acceleration for our laser parameters was (1.1 to 1.5) $\times$ 10^{20} cm^{-3}, as shown in Figure 3. If a short bunch of electrons was trapped near the top of the wave, the monoenergetic beam might be accelerated. Moreover, in order to avoid the mixing of various acceleration field strength, the trail of the plasma wave should be as short as a few wavelengths for the monoenergetic acceleration. The growth rate and the dumping rate as well as the amplitude of the wave should be verified by further experiments.

In order to control the electron injection to the wakefield, the shaped density profile method (Tomassini *et al.*, 2004) and the laser injection (LILAC) method (Umstadter *et al.*, 1996) should be adopted.

5. CONCLUSIONS

Monoenergetic electron beams at 7 to 15 MeV were obtained by focusing 2-TW laser pulses of 50 fs on supersonic gas jets at an intensity of 5 $\times$ 10^{18} W/cm^2 (a_0 = 1.5). The monoenergetic electron beam was accelerated by the moderately large amplitude of a plasma wave. The density of the monoenergetic electron acceleration for our laser parameters was (1.1 to 1.5) $\times$ 10^{20} cm^{-3}. The beam energy was inversely proportional to the electron density in the narrow region. The Stokes satellite peak in the forward scattering well explained the energy spectra of electrons at various plasma densities. Although the wakefield propagated 500 μm, which was well beyond the dephasing length, monoenergetic electron beams were obtained. The divergence angle of the monoenergetic beam was $\pm 1.2°$, which results in the normalized emittance of 0.7 π mm mrad.

We can conclude that monoenergetic beams were accelerated by the wakefield excited by short intense laser pulses; however, some laser-plasma interactions should be confirmed by the further experiments.

ACKNOWLEDGMENTS

This work was financially supported by the Budget for Nuclear Research of the MEXT, based on the screening and counseling by the Atomic Energy Commission and the Advanced Compact Accelerator Development Program of the MEXT.

REFERENCES

Augst, S., Strickland, D., Meyerhoffer, D.D., Chin, S.L. & Eberly, J.H. (1989). Tunneling ionization of noble gases in a high-intensity laser field. *Phys. Rev. Lett.* **63**, 2212–2215.

Bulanov, S.V., Pegoraro, F., Pukhov, A.M. & Sakharov, A.S. (1997). Transverse-wake wave breaking. *Phys. Rev. Lett.* **78**, 4205–4208.

Chen, S.-Y., Krishnan, M., Maksimchuk, A., Wagner, R. & Umstadter, D. (1999). Detailed dynamics of electron beams self-trapped and accelerated in a self-modulated laser wakefield. *Phys. Plasmas* **6**, 4739–4749.

Chen, S.-Y., Krishnan, M., Maksimchuk, A. & Umstadter, D. (2000). Excitation and damping of a self-modulated laser wakefield. *Phys. Plasmas* **7**, 403–413.

Faure, J., Glinec, Y., Pukhov, A., Kiselev, S., Gordienko, S., Lefebvre, E., Rousseau, J.-P., Burgy, F. & Malka, V. (2004). A laser-plasma accelerator producing monoenergetic electron beams *Nature* **431**, 541–544.

Geddes, C.G.R., Toth, C.S., Tilborg, J. Van, Esarey, E., Schroeder, C.B., Bruhwiler, D., Nieter, C., Cary, J. & Leemans, W.P. (2004). High-quality electron beams from a laser wakefield accelerator using plasma-channel guiding. *Nature* **431**, 538–541.

Glinec, Y., Faure, J., Pukhov, A., Kiselev, S., Gordienko, S., Mercier, B. & Malka, V. (2005). Generation of quasi-monoenergetic electron beams using ultrashort and ultraintense laser pulses. *Laser Part. Beams* **23**, 161–166.

Koyama, K., Miura, E., Kato, S., Saito, N., Adachi, M., Kawada, Y., Nakamura, T. & Tanimoto, M. (2003). High-energy electron beam possessing energy peaking at 6 MeV generated by a TW laser pulse with a dense pulsed gas jet. *Bull. Am. Phys. Soc.* **48**, 350.

Koyama, K., Miura, E., Kato, S., Saito, N., Adachi, M., Masuda, M. & Tanimoto, M. (2004). Generation of quasi-monoenergetic high-energy electron beam by plasma wave. *Adv. Accel. Concep., AIP Conf. Proc.* **737**, 528–533.

Kruer, W.L., Dawson, J.M. & Sudan, R.N. (1969). Trapped-particle instability. *Phys. Rev. Lett.* **23**, 838–841.

Malka, V., Fritzler, S., Lefebvre, E., Aleonard, M.-M., Burgy, F., Chambaret, J.-P., Chemin, J.-F. Krushelnick, K., Malka, G., Mangles, S.P.D., Najmudin, Z., Pittman, M., Rousseau, J.-P., Scheurer, J.-N., Walton, B. & Dangor, A.E. (2002). Electron acceleration by a wake field forced by an intense ultrashort laser pulse. *Science*, **298**, 1596–1600.

Malka, V. & Fritzler, S. (2004). Electron and proton beams produced by ultra short laser pulses in the relativistic regime. *Laser Part. Beams* **22**, 399–405.

Mangles, S.P.D., Murphy, C.D., Najmudin, Z., Thomas, A.G.R., Collier, J.L., Dangor, A.E., Divall, E.J., Foster, P.S., Gallacher, J.G., Hooker, C.J., Jaroszynski, D.A., Langley, A.J., Mori, W.B., Norreys, P.A., Tsung, F.S., Viskup, R., Walton, B.R. & Krushelnick, K. (2004). Monoenergetic beams of relativistic electrons from intense laser-plasma interactions. *Nature* **431**, 535–538.

Miura, E., Koyama, K., Kato, S., Saito, N., Adachi, Kawata, Y., Nakamura, T. & Tanimoto, M. (2005). Demonstration of quasi-monoenergetic electron-beam generation in laser-driven plasma acceleration. *Appl. Phys. Lett.* **86**, 251501.

Mori, W.B. & Katsouleas, T. (1992). Ponderomotive force of uniform electromagnetic wave in a time varying dielectric medium. *Phys. Rev. Lett.* **69**, 3495–3498.

Takahashi, T., Sato, T., Yabuuchi, T., Kodama, R., Kotagawa, Y., Ikeda, T., Honda, Y., Okuda, S. & Tanaka, K.A. (2002). Calibration of imaging plate for high energy electron spectrometer (in Japanese). *Ionizing Radiation* **28**, 203–213.

Tanaka, K.A., Yabuuchi, T., Sato, T., Kodama, R., Kitagawa, Y., Takahashi, T., Ikeda, T., Honda, Y. & Okuda, S. (2005). Calibration of imaging plate for high energy electron spectrometer. *Rev. Sci. Instrm.* **76**, 013507.

Tomassini, P., Galimberti, M., Giulietti, A., Giulietti, D., Gizzi, L.A., Labate, L. & Pegoraro, F. (2004). Laser wake field acceleration with controlled self-injection by sharp density transition. *Laser Part. Beams* **22**, 423–429.

Umstadter, D., Kim, J.K. & Dodd, E. (1996). Laser injection of ultrashort electron pulses into wakefield plasma waves. *Phys. Rev. Lett.* **76**, 2073–2074.